GEOMETRIC AND RADIOMETRIC EVALUATION OF THE POTENTIAL OF A HIGH RESOLUTION CMOS -CAMERA

F. Samadzadegan [a], M. Hahn [b], M. Sarpulaki[c,*], N. Mostofi[a]

[a]Dept. of Surveying and Geomatics, Faculty of Engineering, University of Tehran, Tehran, Iran - samadz@ut.ac.ir, mostofi_n@yahoo.com
[b]Dept. of Geomatics, Computer Science and Mathematics, Stuttgart University of Applied Sciences, Stuttgart, Germany – michael.hahn@hft-stuttgart.de
[c]National Cartographic Centre of Iran (NCC), Tehran, Iran - sarpulki@ncc.neda.net.ir

Commission WG III/5

KEY WORDS: Radiometry, Geometry, Accuracy, Close Range, Calibration, Photogrammetry

ABSTRACT:

The progress of digital imaging systems has created manifold opportunities and new applications to close range photogrammetry. The classical techniques have found significant changes and this seems to be an ongoing process which is heavily influenced by new technologies showing up on the sensor market. CMOS (Complimentary Metal Oxide Semiconductor) sensors are on of the challenges to CCD sensors as they are providing a similar performance at a cheaper price level. One of the demands is to investigate the radiometric and geometric characteristics of the imaging sensor. This includes considering other factors involved in image acquisition with CMOS sensors and requires a detailed analysis on the factors and its effects for the overall performance of CMOS cameras. This paper analyses the radiometric and geometric performance of the Canon EOS-1Ds, a high resolution CMOS camera. Presented are issues of restoration and geometric correction as well as an experimental investigation using different Canon EOS-1Ds images. Visual inspection and quantitative analysis of the obtained results demonstrate the high productive capability of the Canon EOS-1Ds camera.

1. INTRODUCTION

For more than 25 years, CCD (Charged Coupled Device) technology was the leading technology in the image sensor industry. With the CMOS technology a competitor to CCD technology has entered the image sensor arena. CMOS (Complimentary Metal Oxide Semiconductor) sensors are challenging the CCD market by providing similar performance in a much cheaper package (Findlater, 2001). Both CCD and CMOS are manufactured in a silicon foundry and the base material and equipments are similar. The main differences are due to architecture, design and flexibility of CMOS that can be integrated on-chip thus leading to a novel family of compact imaging devices.

Figure 1 shows the expected trend in image sensor migration of CCD and CMOS devices for various applications. CCDs will continue to dominate in high-performance, low-volume segments, such as professional digital still cameras, machine vision, medical, and scientific applications. But CMOS will emerge as winner of low-cost, high volume applications, particularly where low power consumption and small system size are key features. From a technical point of view, several criteria are used to evaluate imaging sensors; among them are responsivity, dynamic range, uniformity, speed, and reliability.

Regarding responsivity which is a measure of the signal level of optical energy per unit) CMOS sensors are slightly better than CCDs (Taylor, 1996). Gain stage on-chip and complimentary
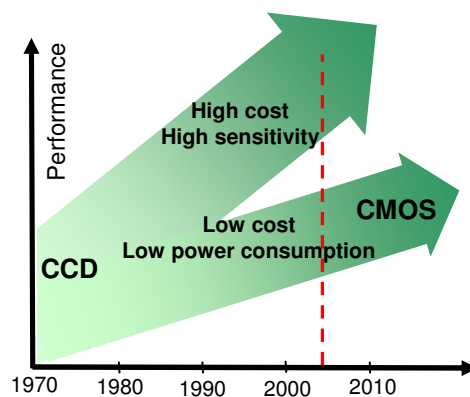
Figure 1. Trend in image sensor migration of CCD and CMOS devices for various applications.

transistors result in relatively high gain with low power consumption of CMOS sensors. CCDs require much more power because the amplification is implemented off-chip. Another category for comparison of the two technologies is its dynamic range. The dynamic range is the ratio of the saturation signal to the noise floor measured at zero exposure. This quantity is much better in CCD technology because it has less on-chip circuitry, which increases the noise immunity of the sensor (Seibold, 2002). External amplification also gives greater control over noise levels. CMOS sensors are more susceptible to uniformity because each pixel has its own amplifier. From a speed point of view, CMOS sensors operate faster because most

---

*Corresponding author.

of the circuitry is on board. This means that signals have less distance to travel and don't have to be piped to other chips on the printed circuit board.

CCDs rely on a process that can leak charge to adjacent pixels when the CCD register overflows; thus bright lights "bloom" and cause unwanted streaks in the image. CMOS architecture is inherently less sensitive to this effect (Table 1). The power consumption of CMOS sensors is at least 10 times smaller that that of similar CCD sensors and CMOS sensors are more durable than CCDs because of the high level of integration on the chip. More integration means less external connection that are susceptible to corrosion and other problems associated with solder joint in harsh environments. It is fairly obvious that CCDs offer greater image quality and noise immunity and are more flexible from a design perspective.

CCD	CMOS
Smallest pixel size	Single power supply
Lowest noise	Single master clock
Lowest dark current	Low power consumption
Established technology market base	Smallest system size
Highest sensitivity	Easy integration of circuity

Table (1) Comparison between CCD and CMOS technology.

The EOS-1Ds has made a huge leap in resolution by means of the continuous development of the CMOS sensor (Figure 2). Canon's CMOS technologies deliver high resolution, low noise and low power consumption, allowing photography to make a quantum leap in terms of digital image quality. Featuring 11.1 effective mega pixels the EOS-1Ds provides the highest image quality with a digital AF-SLR camera. With its extremely high resolution, the EOS-1Ds has been designed to meet the needs of those professional photographers who need the ultimate in digital image quality. Therefore, it could be ideal for professionals active in a wide range of specialties including architectural and industrial photogrammetric photography.

	Professional EOS Digital SLR
	Magnesium body, environmentally sealed, based on EOS-1V
	Integrated battery compartment / vertical hand grip
	11.4 megapixel CMOS sensor (primary colour filter)
	Full frame sensor, no field of view crop / focal length multiplier
	Output image size: 4064 x 2704 or 2032 x 1352

Figure 2. General specification of EOS-1Ds (Cannon 2004)

Various investigations have already been carried out regarding the geometric and radiometric evaluation of digital cameras, no really detailed examination is known for this CMOS camera. Therefore this study investigates the radiometric and geometric potential of the EOS-1Ds CMOS camera.

2. RADIOMETRIC INVESTIGATION

Image restoration describes the removal or reduction of degradations that occurs when the digital image is being generated. These degradations include the blurring that can be introduced by imaging systems, image motion and the noise of electronic or electromagnetic sources. In other words,

restoration attempts to reconstruct or recover an image that has been degraded by using a prior knowledge of the degradations (Castleman, 1996; Gonzalez and Woods, 2002).

2.1 Model of Degradations

Figure 3 illustrates the process of how a degraded image $g(x, y)$ is formed by blurring an ideal image $f(x,y)$ with a system operation $h(x, y)$ followed by adding noise $n(x, y)$:
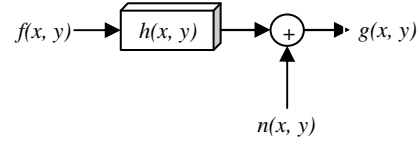
Figure 3. Model of degradation

If $h(x,y)$ is a linear, position-invariant process, then the degraded image is given by:

$$g(x, y) = h(x, y) * f(x, y) + n(x, y) \qquad (1)$$

Here, (*) indicates convolution.

2.2 Model of Wiener Deconvolution Filter

For restoration of CMOS images, both the degradation function and statistical characteristics of noise should be considered. Wiener Deconvolution is based on considering images and noise as random processes. The objective is to get an estimate of the uncorrupted image is such away that the mean square error between degraded and undegraded images is minimized. Further, it is assumed that noise and image are uncorrelated, and the gray levels in the estimated image are a linear function of the levels in the degraded image (Castleman, 1996; Gonzalez and Woods, 2002). By these assumptions, the Wiener deconvolution filtering in frequency domain reads as follows:

$$\hat{F}(u,v) = \left[\frac{H*(u,v)}{|H(u,v)|^2 + P_n(u,v)/P_f(u,v)} \right] G(u,v) \qquad (3)$$

where $\hat{F}(u,v)$ is the restored image, $H(u, v)$ is degradation function (OTF), $H*(u,v)$ is complex conjugate of $H(u, v)$, $P_n(u,v) = |N(u,v)|^2$ is power spectrum of the noise and $P_f(u,v) = |F(u,v)|^2$ is power spectrum of the undegraded image.

An approach used frequently when the quantities of $P_n(u,v)$ and $P_f(u,v)$ can not be estimated is to approximate Equation 3 by the expression:

$$\hat{F}(u,v) = \left[\frac{H*(u,v)}{|H(u,v)|^2 + K} \right] G(u,v) \qquad (4)$$

where K is a constant (Gonzalez and Woods, 2002).

In the follooing, we propose an approach for estimating the system degradation model and noise of CMOS images and then, by designing a Wiener deconvolution filter, we attempt to restore a CMOS image which is corrupted by degradations.

2.3 Determination of Noise and PSF

The first step for determining noise and point spread function (PSF) of the system is to provide ideal (rectangular) targets, to

achieve a good estimate of both. The CMOS image of such a target is shown in Figure 4.
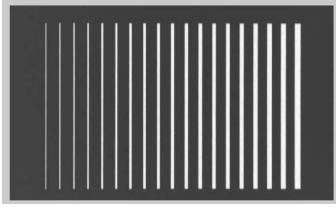
Figure 4. Digital CMOS image of an ideal target

The second step is to select a patch of one of the individual targets (rectangles), that includes two vertical edges (Figure 5).

Figure 5. One of the edge targets (left) and corresponding picked up patch

The third step is to reduce the noise in the above selected image patch by applying a low-pass filter, for example an averaging filter with a 5x5 window (Figure 6).
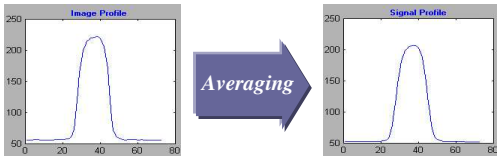
Figure 6. Image (left) and signal (the data without noise) profiles (right).

By subtracting the result of averaging filter from its corresponding image patch, the noise profile is achieved, as shown in Figure 7:

Figure 7. Left: Signal profile (result of lowpass filter), Right: Noise profile.

Now, a Wiener filter should be applied to the image patch to a create a profile, which just contains the system blur effect. By fitting a rectangle (Figure 8), which indicates the ideal signal profile, on the profile of Wiener filter, the PSF of the CMOS system can be calculated in frequency domain by the expression:

$$H_{(OTF)} = \frac{FT(SP)}{FT(RP)} \qquad (5)$$

Where $H_{(OTF)}$ is OTF (Fourier transform of the 1-D PSF), $FT(SP)$ is Fourier transform of the signal profile and $FT(RP)$ is Fourier transform of the rectangle profile.
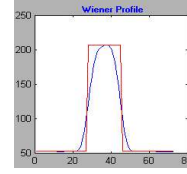
Figure 8. Fitting a rectangle on Wiener profile

Now, by fitting a proper 1-D Gaussian to the PSF profile, the oscillations of PSF will be reduced. The total PSF of the system will be achieved by expanding the 1-D Gaussian function to the 2-D Gaussian function:
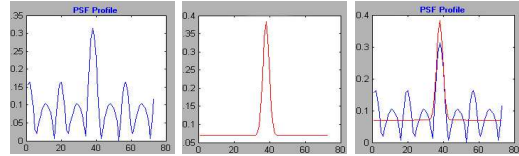
Figure 9. PSF profile (left), Gaussian function (middle), fitted Gaussian function to PSF profile (right).

2.4 The Wiener Deconvolution Filter

By using the calculated PSF and noise to signal power ratio (K), the Wiener deconvolution filter can be calculated by using Equation 4. The size of this filter should be expanded to the size of the image patch, which is to be restored (Stockam, et. al, 1975).

2.5 Experiments and Results

To evaluate the proposed restoration process, the estimated PSF is used for radiometric correction of an outdoor image (Figure 10). Visual comparison of the obtained result with the input image demonstrates the capability of the applied restoration strategy.

Figure 10. Initial image (above) and the restored image generated by Wiener deconvolution (below).

3. GEOMETRIC INVESTIGATION

Although a CMOS array is mechanically quite stable and the pixels have a fixed geometric relationship, the use of these imaging systems for metrology purposes requires calibrating or checking of these camera systems. Online calibration of cameras during data collection process is possible for many types of photogrammetric work, but offline calibration and checking is more recommendable in the following cases:

- When information is desired about the attainable accuracy of the measurement system and thus about the measurement accuracy at the object;
- when online calibration of the measurement system is almost impossible for system immanent reasons so that some or all other system parameters have to be predetermined;
- when complete imaging systems or components are to be tested by the manufacturer for quality-control purposes;
- when digital images free from the effects of the imaging system are to be generated in preparation of further processing steps (such as rectification).

When setting up measurement systems it will be necessary to determine the position of cameras or other sensors in relation to a world coordinate system to allow 3D determination of objects within these systems.

3.1 Mathematical Modelling for Calibration of a CMOS Camera

There are several mathematical models for offline calibration of geometric structure of the present CMOS system (Ehlers, 1997; Madani, 1999). These formulations conceptually can be divided into two main groups: *Rigorous Sensor Models* (RSMs) and *Generic Sensor Models* (GSMs).

RSMs reconstruct the spatial relations between sensor and object based on using conventional colinearity equations. The method is highly suited to frame type sensors and non-linear effects caused by lens distortion. Film deformations are modelled by additional parameters or by corrections after the linear transformation. Such image-specific parameters often include the approximate sensor position coordinates and sensor attitude angles. As RSMs basically are nonlinear models, the linearization and the requirement for suitable initial values of the unknowns are inevitable. Therefore there is a need for alternative approaches in case that we could not easily apply the RSMs.

GSMs are presented as a sophisticated solution for overcoming the RSMs limitations. Although GSMs have been adopted a decade ago (Paderes et. al, 1989; Greve, 1992), the attempts to study both theoretical properties and empirical experimental results have started to appear only recently and are still rarely reported.

In this study the tests are conducted based on evaluation of several different generic mathematical models, e.g. 2D Projective, 3D Affine, Rational function (Atkinson K.B., 1996) models for offline calibration of Canon EOS-1Ds CMOS camera.

- **Projective Transformation**

  The projective transform describes the relationship between two planes. It is defined by eight parameters, which can be derived from four object points lying in a plane and their corresponding image coordinates.

  $$x = \frac{a_1 X + a_2 Y + a_3}{c_1 X + c_2 Y + 1}$$

  $$y = \frac{b_1 X + b_2 Y + b_3}{c_1 X + c_2 Y + 1}$$

  Where x, y are coordinates of points in original image; X, Y are coordinates of points in object space; and $a_1, a_2, a_3, b_1, b_2, b_3, c_1, c_2$ are projective parameters.

- **3D Affine Transformation**

  The model for 3D analysis of linear array imagery via a 3D affine model is given by Hattori (2000).

  $$x = a_1 X + a_2 Y + a_3 Z + a_4$$

  $$y = b_1 X + b_2 Y + b_3 Z + b_4$$

  Where x, y are coordinates of points in original image; X, Y, Z are coordinates of points in object space; and a_1 to b_4 are affine parameters.

- **Rational Functions**

  The RFM uses a ratio of two polynomial functions to compute the x coordinate in the image, and a similar ratio to compute the y coordinate in the image.

  $$x = \frac{\sum_{i=0}^{m_1}\sum_{j=0}^{m_2}\sum_{k=0}^{m_3} a_{ijk} X^i Y^j Z^k}{\sum_{i=0}^{n_1}\sum_{j=0}^{n_2}\sum_{k=0}^{n_3} b_{ijk} X^i Y^j Z^k}, \quad y = \frac{\sum_{i=0}^{m_1}\sum_{j=0}^{m_2}\sum_{k=0}^{m_3} c_{ijk} X^i Y^j Z^k}{\sum_{i=0}^{n_1}\sum_{j=0}^{n_2}\sum_{k=0}^{n_3} d_{ijk} X^i Y^j Z^k}$$

  x, y are normalized pixel coordinates on the image; X, Y, Z are normalized 3D coordinates on the object, and a_{ijk}, b_{ijk}, c_{ijk}, d_{ijk} are polynomial coefficients. The polynomial coefficients are called rational function coefficients (RFCs).

3.2 Experiments and results

To assess the geometric stability of Canon EOS 1-Ds images, a images from a calibration environment have been taken (Figure 11). With large amount of control and check points visible in the image (Figure 11) the selected area can be well used for the evaluation of the geometric parameters if interest.
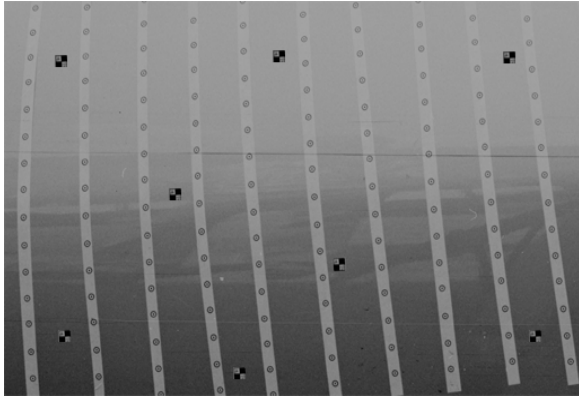
Figure 11. A patch of the calibrated data set.

All the three models presented above are applied to this calibration data set. The vector plot of the residual errors for GCPs and the check points for all mathematical models are displayed in Figure 12.

RMSE on control points = 9.51
RMSE on check points = 10.06
15 micron

Projective Transformation

RMSE on control points = 8.19
RMSE on check points= 9.14
15 micron

3D Affine Transformation

RMSE on control points = 2.14
RMSE on check points = 2.51
15 micron

Rational Function (Order 3 with full terms)
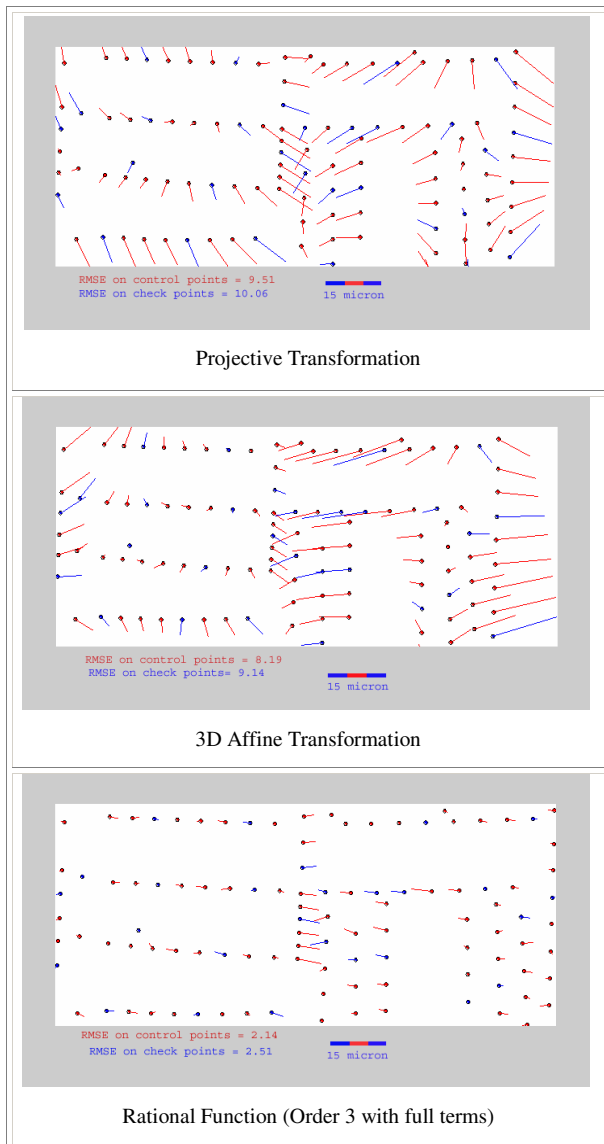
Figure 12. Vector plot of residual errors of the different mathematical models.

These graphs indicate that:

1. Projective transformation is stable as regards the error fluctuations. However, it seems not to be flexible enough to take care of the inherent non-linearity of the image distortions.

2. The 3D affine transformation has the same limitation as the projective transformation.

3. The rational functions show a good performance in particular if the coefficients for the denominators are selected to be the same for the X and Y components.

4. Although quite flexible, polynomials and rational functions main shortcomings are their non-stability for the position of the points located between GCPs. The error can be drastically amplified for those points that are far from the GCPs. That is, GCPs distribution plays a decisive rule in retaining the model stability.

5. Apart from polynomials, increasing the number of GCPs increases the fitting and absolute accuracy. However, the accuracy figures do not show a clear improvement if the number of GCPs are increased beyond certain levels.

4. CONCLUSION REMARKS

In this study the following experiments have been conducted to analyze the radiometric and geometric performance of Canon EOS-1Ds high resolution CMOS camera.

To evaluate the radiometric potential of CMOS, the point spread function (PSF) of the imaging system was estimated. This was done by using the smallest detectable symmetric feature with a uniform grey scale background that could be found in the image. The sigma of the PSF was determined by assuming a Gaussian model for it. The pictorial restoration operations were then performed by modified inverse and Wiener filters respectively.

Geometric correction of the CMOS camera has been examined based on an evaluation of three mathematical models based on Rational functions, 3D Affine and 2D Projective transformation. For the accuracy evaluation vector plots of the residual errors for control points and check points are prepared.

Further experiments with other Canon EOS-1Ds images confirm the high capability of this CMOS camera.

5. REFERENCES

Atkinson, K.B., 1996. Close Range Photogrammetry and Computer Vision,Whittles Publishing Bristol.

Castleman, K.R., 1996. *Digital Image Processing*, Prentice-Hall, Simon&Schuster.

Cannon, 2004: http://www.canon.co.uk/For_Home/Product_Finder/Cameras/Digital_SLR/EOS_1Ds/

Dowman, I., and J.T. Dolloff, 2000. An evaluation of rational functions for photogrammetric restitution. Int'l Archive of photogrammetry and Remote Sensing, 33(Part B3): 254-266.

Findlater, K.M., 2001. A CMOS camera employing a double junction active pixel, University of Edinburgh.

Greve, C.W., Molander, D., Gordon, K., 1992. Image processing on open systems, PE&RS, 58(1): 85-89.

Gonzalez, R.C., Woods, R., 1993. *Digital Image Processing*, Addison Wesley Publishing Massachusetts.

Madani, M., 1999. Real-time sensor-independent positioning by rational functions. Proceeding of ISPRS Workshop on Direct versus Indirect Methods of Sensor Orientation, 25-26 November 1999, Barcelons, Spain, pp. 64-75.

Paderes, Jr, F.C., E.M. Mikhail, and J.A. Fagerman, 1989. Batch and on-line evaluation of stereo SPOT imagery. *Proceeding of the ASPRS-ACSM Convention*, 02-07 April, Baltimore, Maryland, pp. 31-40.

Seibold C., 2002. Comparison of CMOS and CCD Image Sensor Technologies. ECE 442 Senior Design, 2002.

Stockam, T.G., Cannon, T.M., Ingebretsen, R.B., 1975 . Blind deconvolution through digital signal processing, *Proceedings of the IEEE*, Vol: 63 No. 4, pp. 678–692.

Tao, C. V., and Y. Hu, 2001. A comprehensive study of the rational function model for photogrammetric processing. Photogrammetric Engineering & Remote Sensing, 67(12): 1347-1357.

Taylor, S. A., 1998. CCD and CMOS Imaging Array Technologies: Technology Review. Technical report. Cambridge, UK.